Searches for Cosmic Ray Electron Anisotropies with the *Fermi*-Large Area Telescope

Vlasios Vasileiou

CNRS/IN2P3 &

Laboratoire Univers et Particules de Montpellier

and

M. N. Mazziotta

INFN, Bari

for the *Fermi*-LAT collaboration

Motivation

- The Galactic Magnetic Field (GMF) isotropizes the direction distribution of GeV-TeV CRs → direction information of CR sources is lost.
- Compared to hadronic Cosmic-Rays, CREs lose their energy rapidly.
  - 100 GeV (1TeV) CREs detected at the earth have originated ***from relatively nearby locations*** at most ~1.6 (0.75) kpc away.
  - Likely to have ***originated from an anisotropic collection of few nearby sources***.
  - Depending on the propagation through the GMF, some anisotropy in the directions of GeV-TeV CREs might still exist.
- Remember: Past studies tried to quantify the effect of nearby older pulsars to the detected CRE spectra and to the CR-Positron fraction (e.g. Geminga, Monogem).
  - They predicted anisotropies towards the directions of dominant sites of CRE production.
  - ***The discovery of an anisotropy in agreement with the predictions of these studies would help us towards revealing the sources of CREs.***

The Large Area Telescope

- **Tracker**
  - Measures the direction, primary ID
- **Imaging Calorimeter**
  - Measures the energy, primary ID, (also helps with direction rec.)
- **Segmented anti-Coincidence Shield**
  - Identifies charged Cosmic Rays
- Primarily conceived as a detector for 20MeV->300GeV gamma rays.
- However, it can be also used as a detector for Cosmic Ray Electrons and Positrons (hereafter CREs).

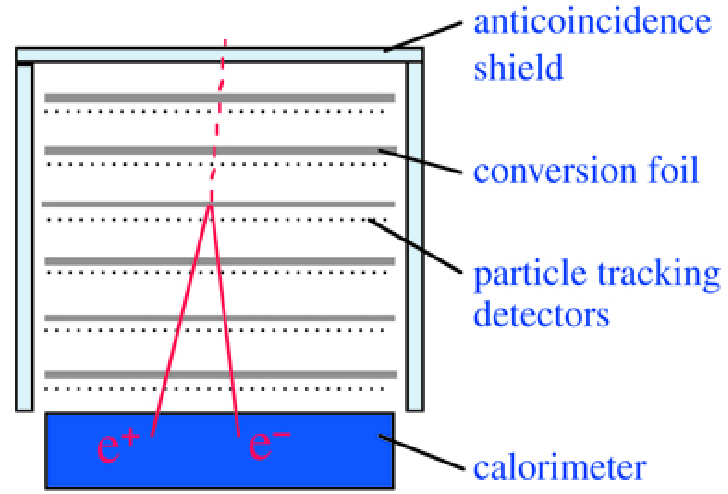

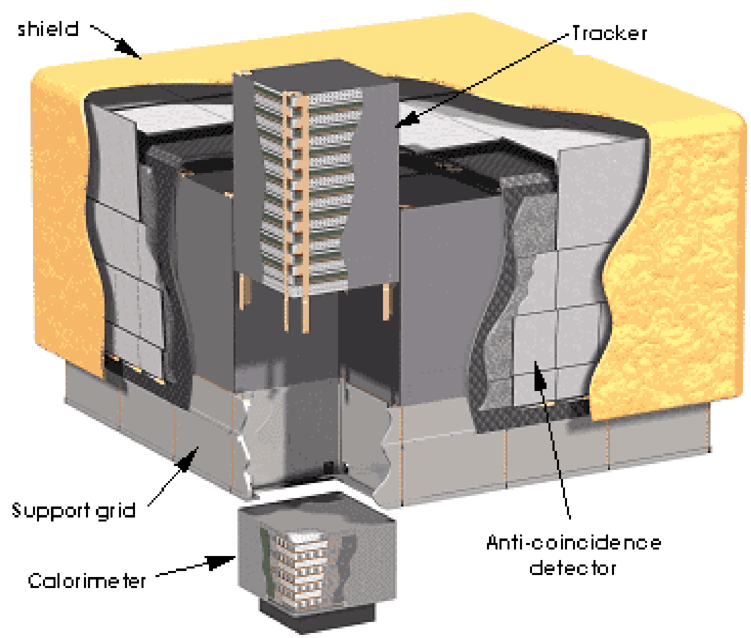

Event Display – EM vs hadronic events

- The event selection is performed using information from all the LAT subsystems: tracker, calorimeter, and ACD.
- Selection between EM and hadronic events is based on the different event topologies – most powerful separator is the lateral profile of the shower.
- Photons are identified using the absence of signal from the ACD

Electron candidate 844 GeV

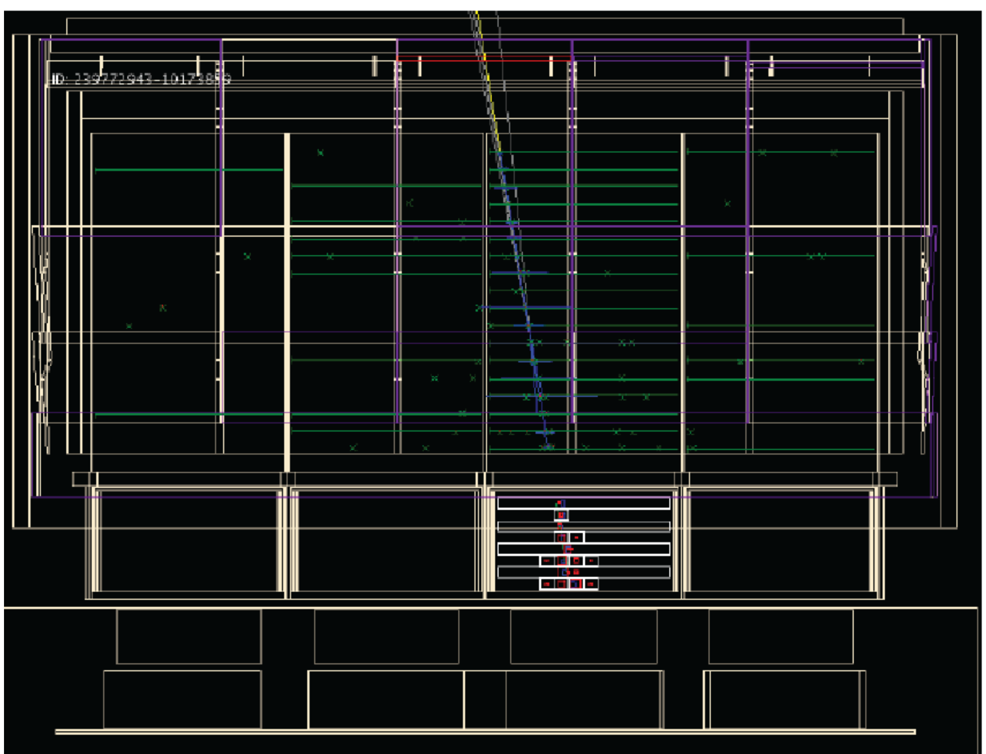

Background event, 765 GeV

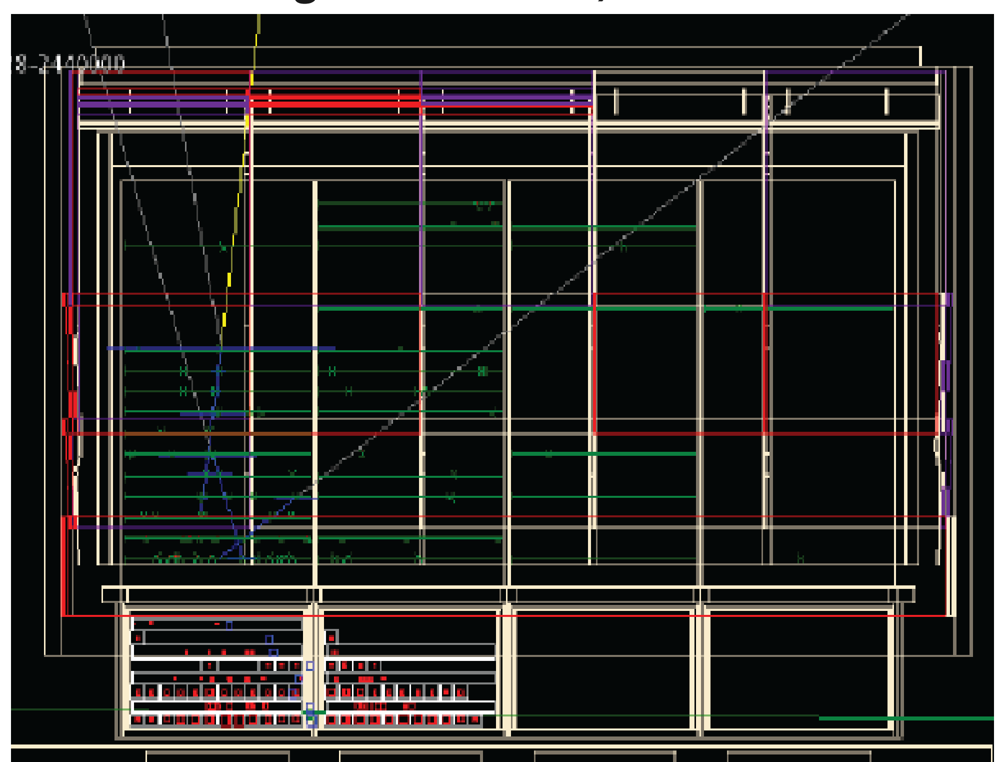

Dataset

- 1yr worth of data taking (starting August 2008)
- 1.35 million events with energies E>60GeV
- ~0.1° angular resolution, ~10% energy resolution
- Low contamination:
  - Photons → <0.1%
  - Hadronic CRs → ~13% (projected anisotropy under our sensitivity)
- Whole-sky coverage (survey-mode data)
  - Allows us to search for anisotropies of ***any angular size (up to dipole) and from any direction in the sky***.

Analysis Overview

- We searched the data for anisotropies ***without any a priori assumptions on the energy, angular size, and direction of the possibly anisotropy***.
  - Analyzed different data subsets:
    - E>60GeV, E>120GeV, E>240GeV, E>480GeV.
  - Each subset was searched for anisotropies with angular scales ranging from ~10^{o} to 90^{o} (dipole) in radius.
- **Multiple search methods:**
  - Search for very small effects (fraction of a percent).
  - Used multiple analysis methods as a cross-check for any systematics and to maximize the sensitivity.

Analysis Overview – The Method

1. **Construction of the "no-anisotropy skymap"**:
   - Calculated how the sky would look like on average (for our 1-year observation) if the CRE direction distribution was perfectly isotropic.
   - By comparing this "no-anisotropy skymap" to the actually-detected skymap we searched for the presence of any anisotropies in the data.
   - We used two techniques to construct the no-anisotropy skymap:
     - "Event-Shuffling" and "Direct-Integration" techniques.
     - Both rely solely on the data → No dependence on the LAT's MC.
     - ✔ *The results of the two techniques were consistent with each other.*
2. **Comparison of the no-anisotropy to the actual skymap**: Two methods to accomplish that:
   a) Direct bin-to-bin comparison between the two skymaps.
   b) A spherical harmonic analysis of "fluctuation maps" (maps produced by dividing the actual by the no-anisotropy skymap).

Event-Shuffling Technique

- Starts from the original data set and randomly shuffles the reconstructed directions of events (in the instrument frame).
  - The reconstructed energy and direction distributions (in the instrument frame) remain the same.
  - However, ***any anisotropy in sky coordinates is smeared out.***
- The randomization process is repeated multiple times (100), with each iteration producing a skymap that is statistically consistent with the case of an isotropic CRE direction distribution.
- These skymaps are then averaged, to construct the final no-anisotropy skymap.
- The technique is simple to implement and straight forward. It also has the benefit of automatically taking care of any short-term variations of the detector's effective area.

Direct-Integration Technique

- In general, the rate of events from some direction in instrument coordinates (θ,φ) is equal to the all-sky rate $R_{allsky}(t)$ times the probability that an event is reconstructed at that direction $P(\theta,\varphi,t)$.
- Based on the above, given a value for these two variables and the pointing information of the instrument, we can construct an associated skymap.
- What we want to do is to find the value of these variables that corresponds to the case of a perfectly isotropic CRE direction distribution, and using this value construct the no-anisotropy skymap. Which is this value?

✗ As an anisotropy passes through the LAT's FOV, it creates fluctuations in the ***instantaneous value*** of these variables.

✔However, their ***averaged-over-multiple-orbits value*** remains constant, since any anisotropy events are averaged out.

Some Independent-Bin Skymaps

- **Top**: A no-anisotropy skymap constructed with the Event Shuffling technique for E>60GeV.
- **Bottom**: The E>60GeV actual signal skymap.
- Each map contains 12,288 ~1° independent bins (HealPix pixelization).
- The variations in the maps are due to the non-uniform exposure.

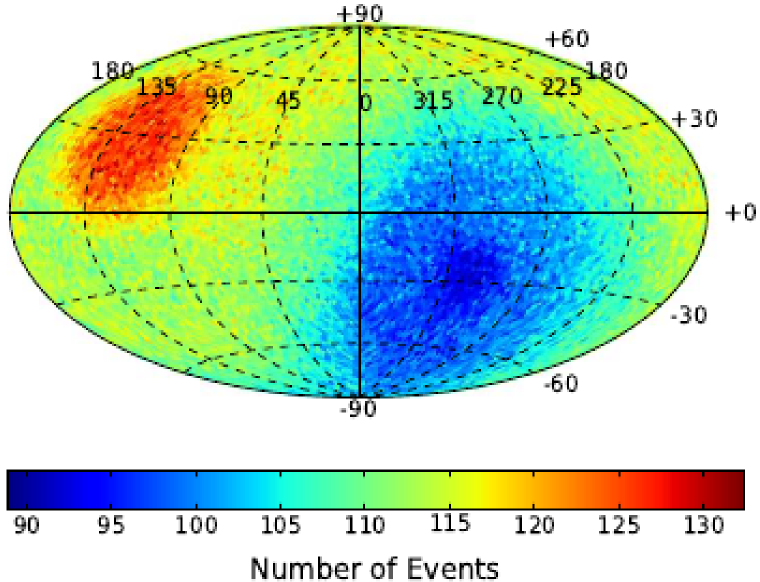

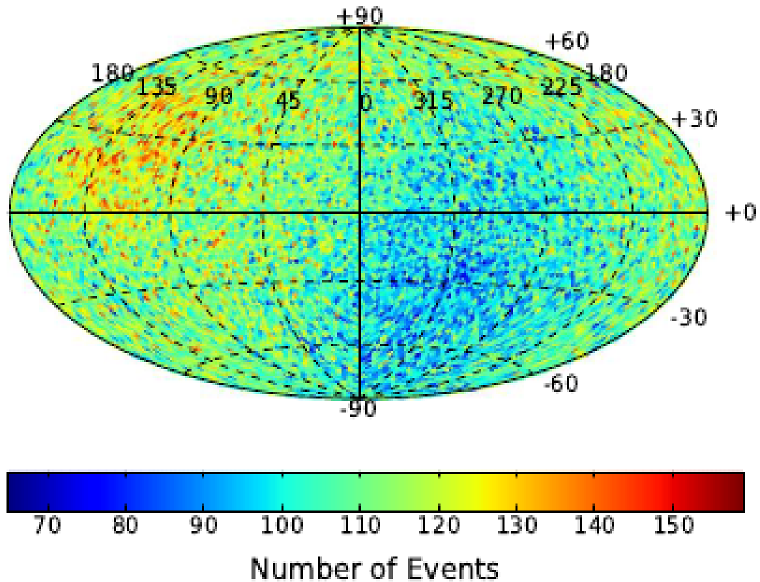

Direct Bin-to-Bin Comparison

- **First method:** Direct bin-to-bin comparison between the constructed no-anisotropy and the actual skymap. Two step process:

1. **Map Integration:**
   - Searching for tens-of-degrees wide anisotropies using 1° independent-bins maps is highly inefficient.
   - We integrated the no-anisotropy and signal independent-bins maps to produce pairs of skymaps corresponding to various integration radii (10°, 30°, 45°, 60°, 90°).
2. **Bin-to-bin Comparison:**
   - For each pair of bins in the actual and the no-anisotropy skymap with contents $n_{Sig,i}$ and $n_{Iso,i}$ respectively, we calculated the probability of detecting a number of events at least as small as $n_{Sig,i}$ while expecting $n_{Iso,i}$.
   - For the Event-Shuffling technique maps we used Li & Ma significances. For the Direct-Integration technique maps we used simple Poisson probabilities.

Sample Significance Maps

- E>60GeV
- 10º,30º,45º,60º,90º integration radius
- Pre-trials significances

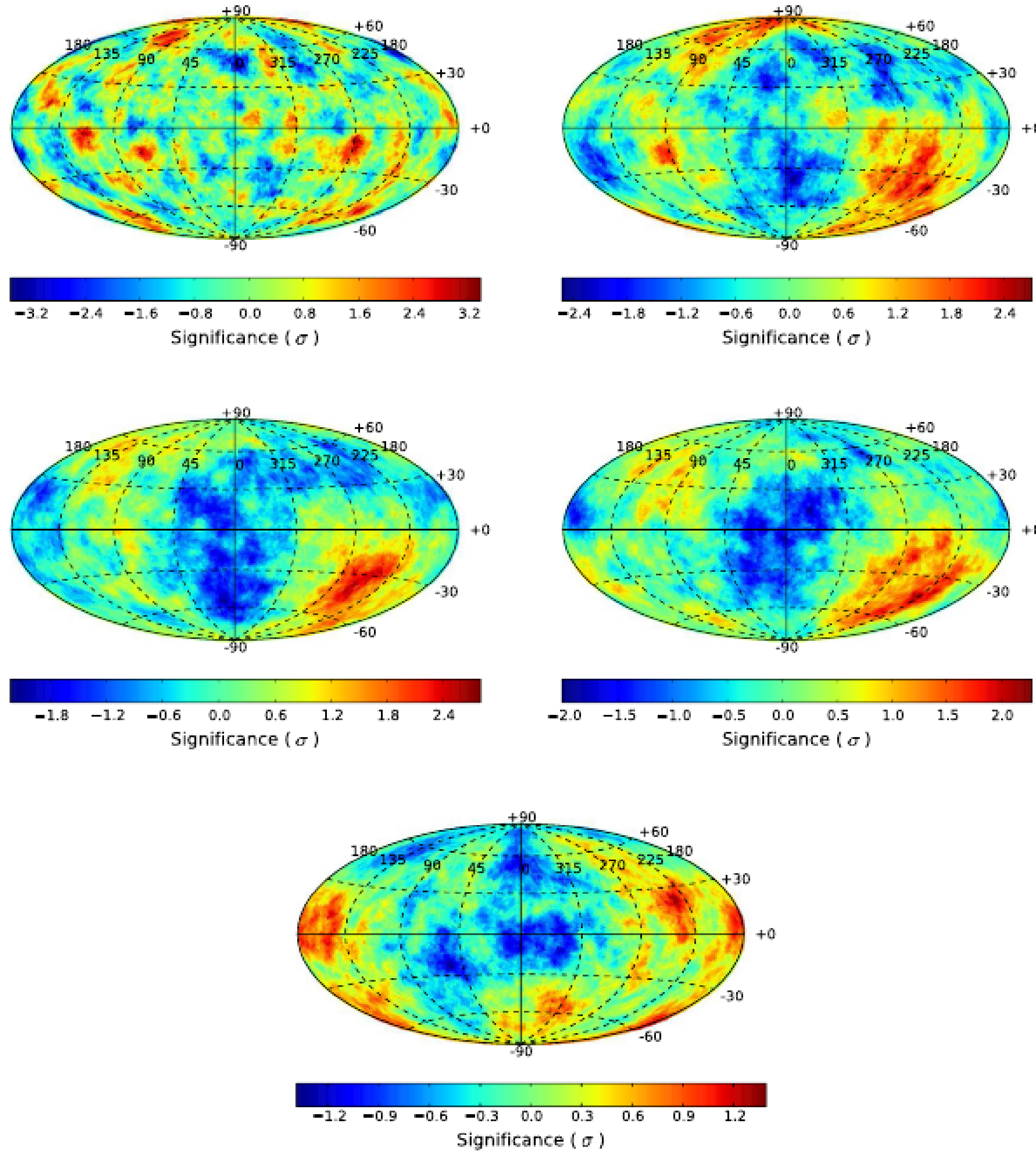

Example Integrated Significance Maps

Event Shuffling

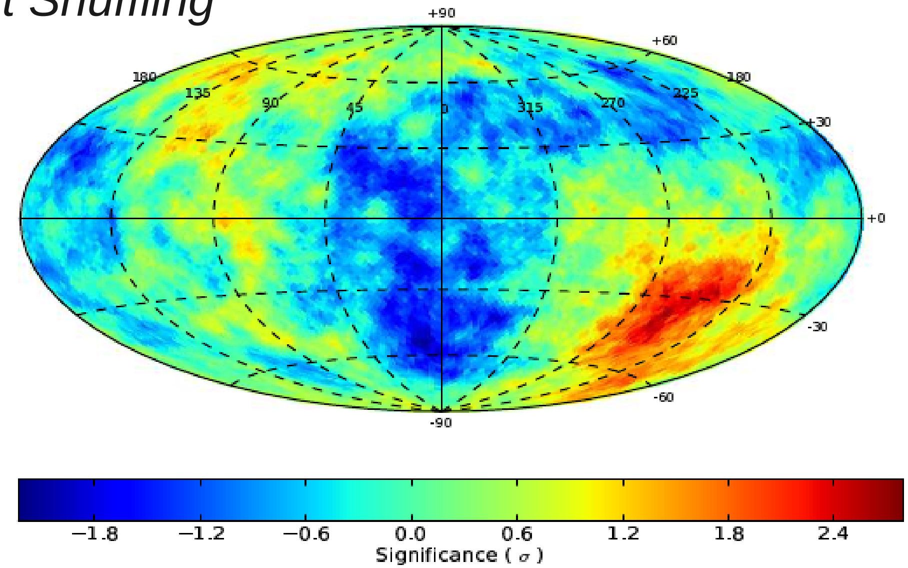

Direct Integration

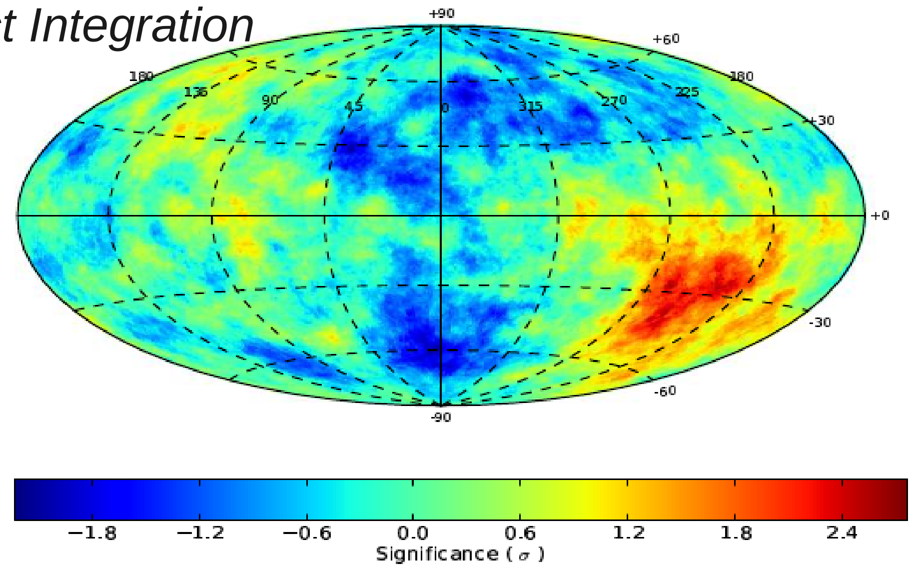

- Significance maps produced by comparing the pairs of integrated no-anisotropy and actual skymaps.
- E>60GeV, 45^{o} integration
- The results of the two techniques were consistent with each other.

➢ *These are pre-trials significances.*

Effective number of trials

- **Curves:** Effective number of trials involved in evaluating each of the the 12,288 possible directions in an integrated significance skymap.

- The larger the integration radius the smaller the effective number of trials.
- These data were produced by simulating randomized significance skymaps and counting the fraction of such skymaps (P_{post}) that a probability less or equal than (P_{pre}) was found.

$$T_{eff} = \frac{log(1 - P_{post})}{log(1 - P_{pre})}.$$

$$P_{post} = 1 - (1 - P_{pre})^{T_{eff}}.$$

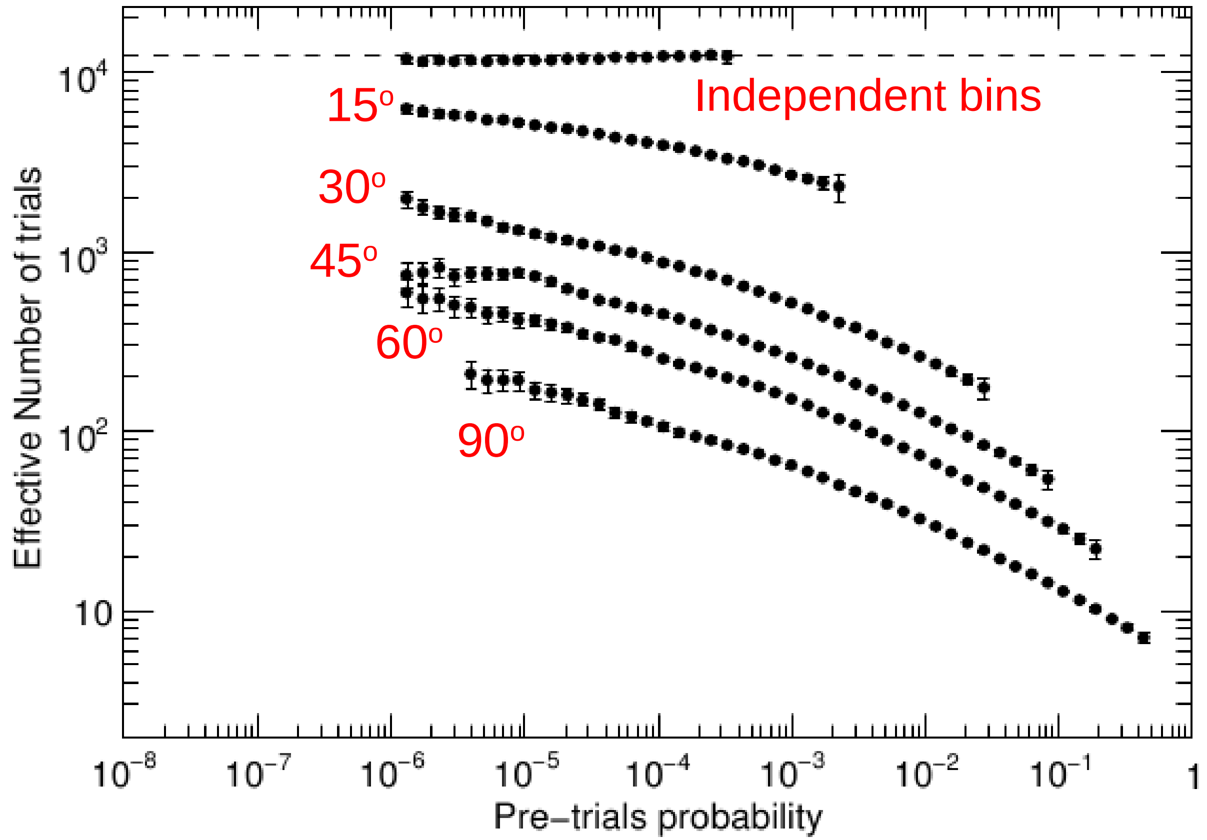

Sensitivity of the Bin-to-Bin Search

- From the effective number of trials and the number of events in the dataset we can calculate the sensitivity of this method.
- **Markers**: Sensitivity of the bin-to-bin search – fractional excess needed to detect an anisotropy with a post-trials significance 3σ.
- Ignore the curves for now

- Sensitivity worse for smaller integration radii (large effective number of trials) and for higher energies (fewer detected events).
- Most sensitive for E>60GeV and for a dipole anisotropy: ~fraction of a percent

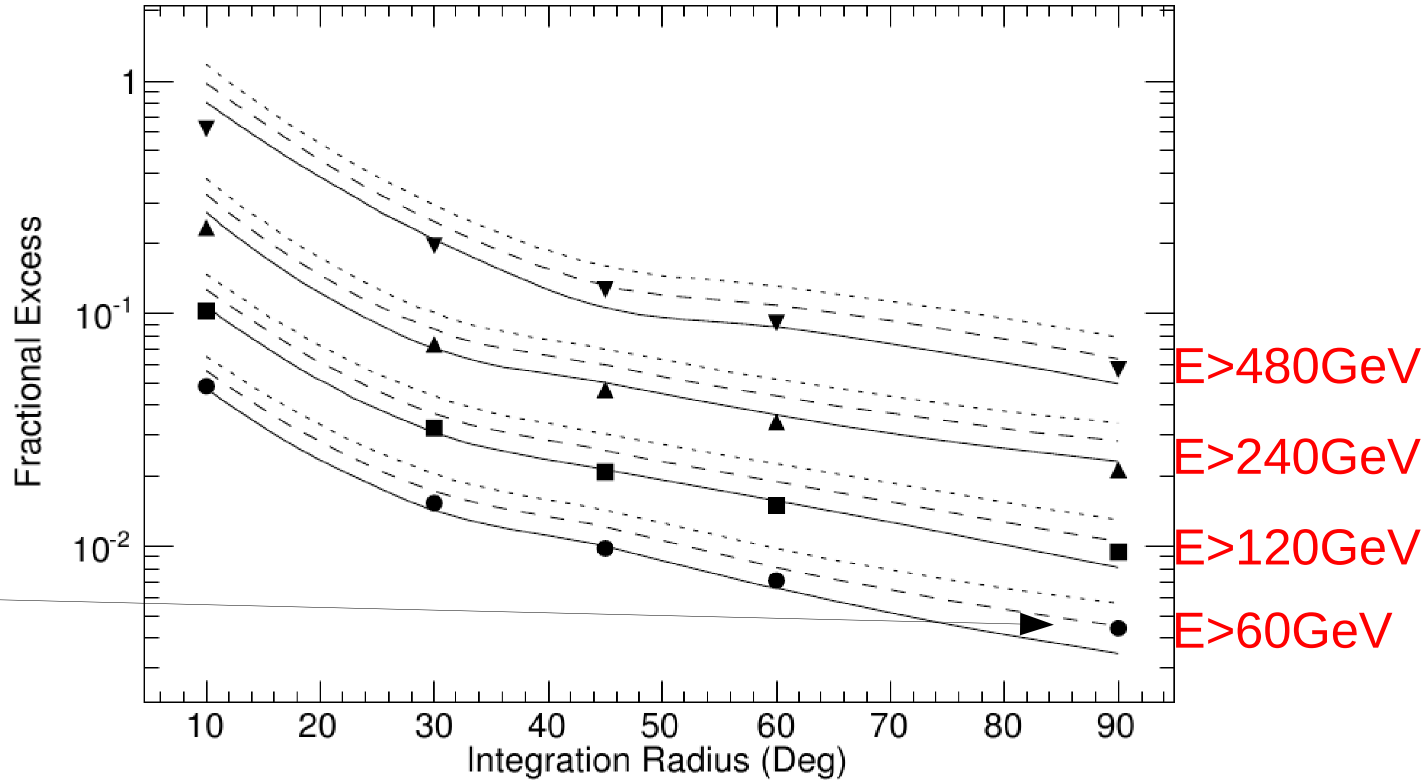

Pre- and post-trials significances

- **Curves:** correspondence between a pre and a post-trials significance (connected through T_{eff}).
- **Markers:** highest post-trials significance in each of the different tests (one for each E_{min} and integration radius).
- **All the results are post-trials insignificant.**

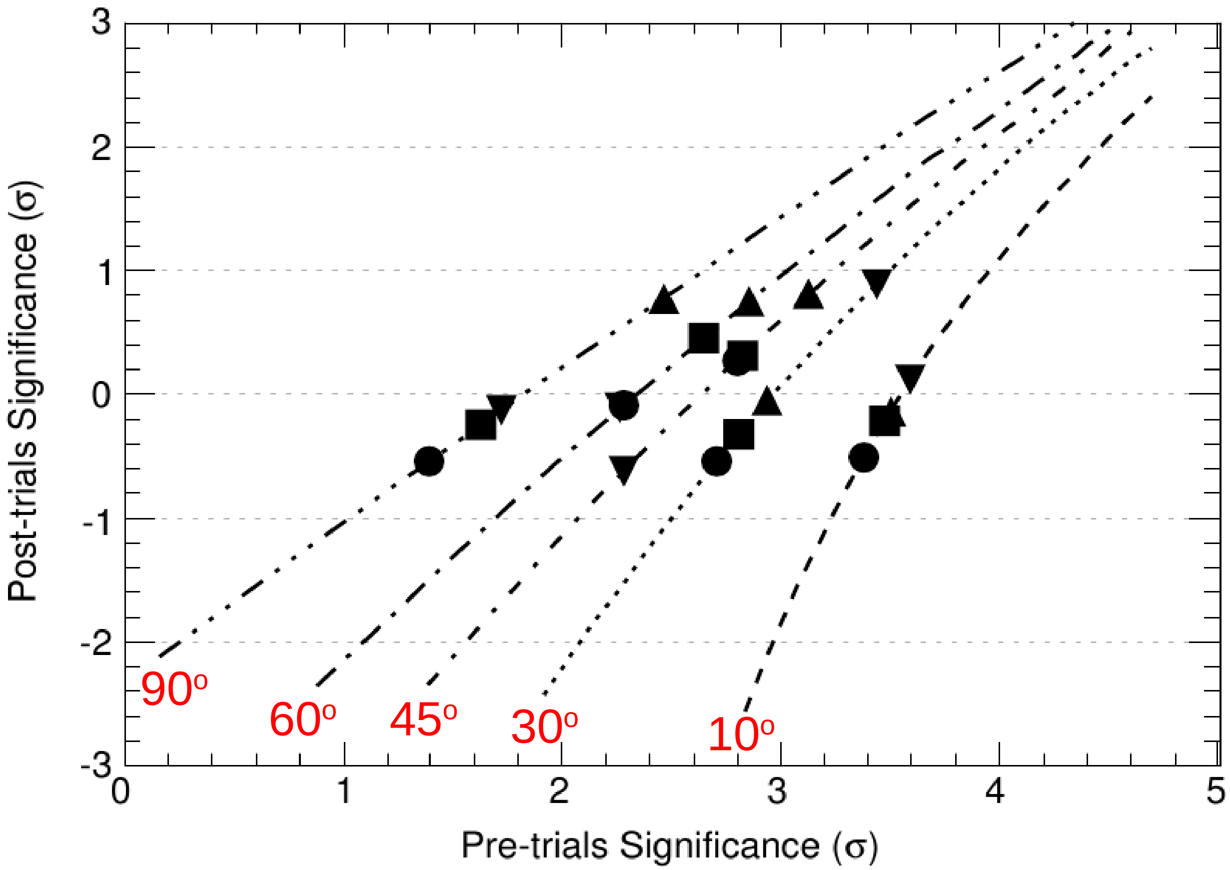

Upper limits on the fractional excess

- **Curves**: 1-2-3σ upper limits on the fractional excess, for the bin-to-bin search.
- **Markers**: Sensitivity of the bin-to-bin search.

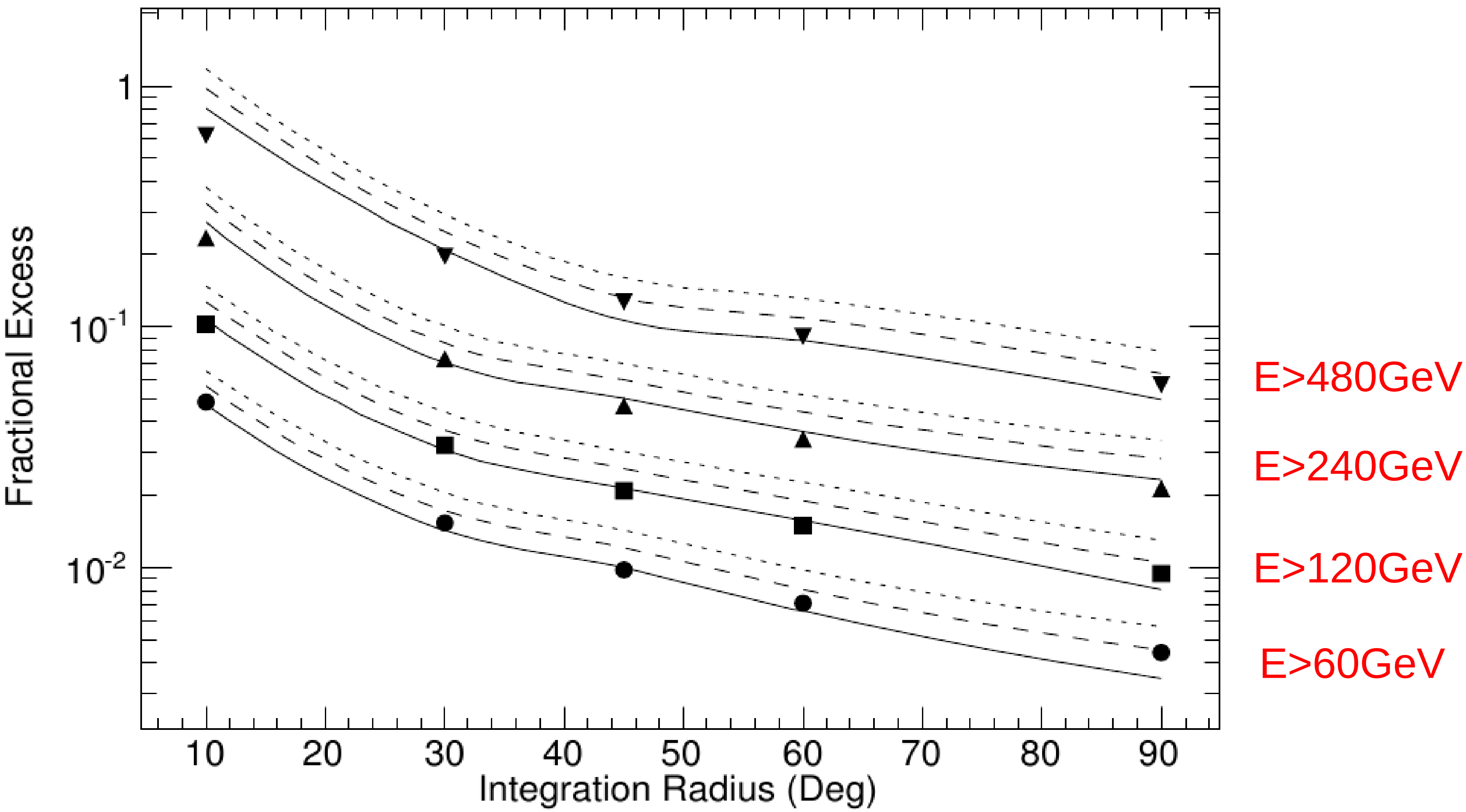

Significance at interesting Locations

- Also checked the significance towards
  - Vela, Geminga, and Monogem pulsars,
  - Virgo and Cygnus regions
  - Galactic and anti-galactic Center.
- Such a search involves a considerably smaller number of trials → higher sensitivity.
- Best post-trials significance towards the anti-galactic center (1.5σ) → not significant.

Method #2. Spherical Harmonic Analysis

- Spherical harmonic analysis of a "fluctuation map" equal to the ratio of signal over the no-anisotropy skymap minus one.
- The fluctuation map was expanded in the basis of spherical harmonics, producing a set of a_{lm} coefficients.
- The average variance of these coefficients was used to construct the angular power spectrum:

$$\hat{C}_l = \frac{1}{2l+1} \sum_{m=-l} |a_{lm}|^2 .$$

- An increased power at a multipole *l* would correspond to the presence of an anisotropy in the data would angular scale ~180°/*l*.
- To judge whether the observed spectrum showed any significant signs of anisotropy, we compared it to the power spectrum of an isotropic signal.
  - Power spectrum of an isotropic dataset known → behaves as white noise.
  - White-noise power spectrum: power at a multipole *l* follows a χ^2_{2l+1} distribution centered at 4π/N (where N is the total number of events).

Power Spectra

- **Markers**: Power spectra from both the ES and DI techniques (dots, squares resp.).
- **Curves:** Ranges that show the 2σ and 3σ integrated-probability fluctuations of a white-noise spectrum.

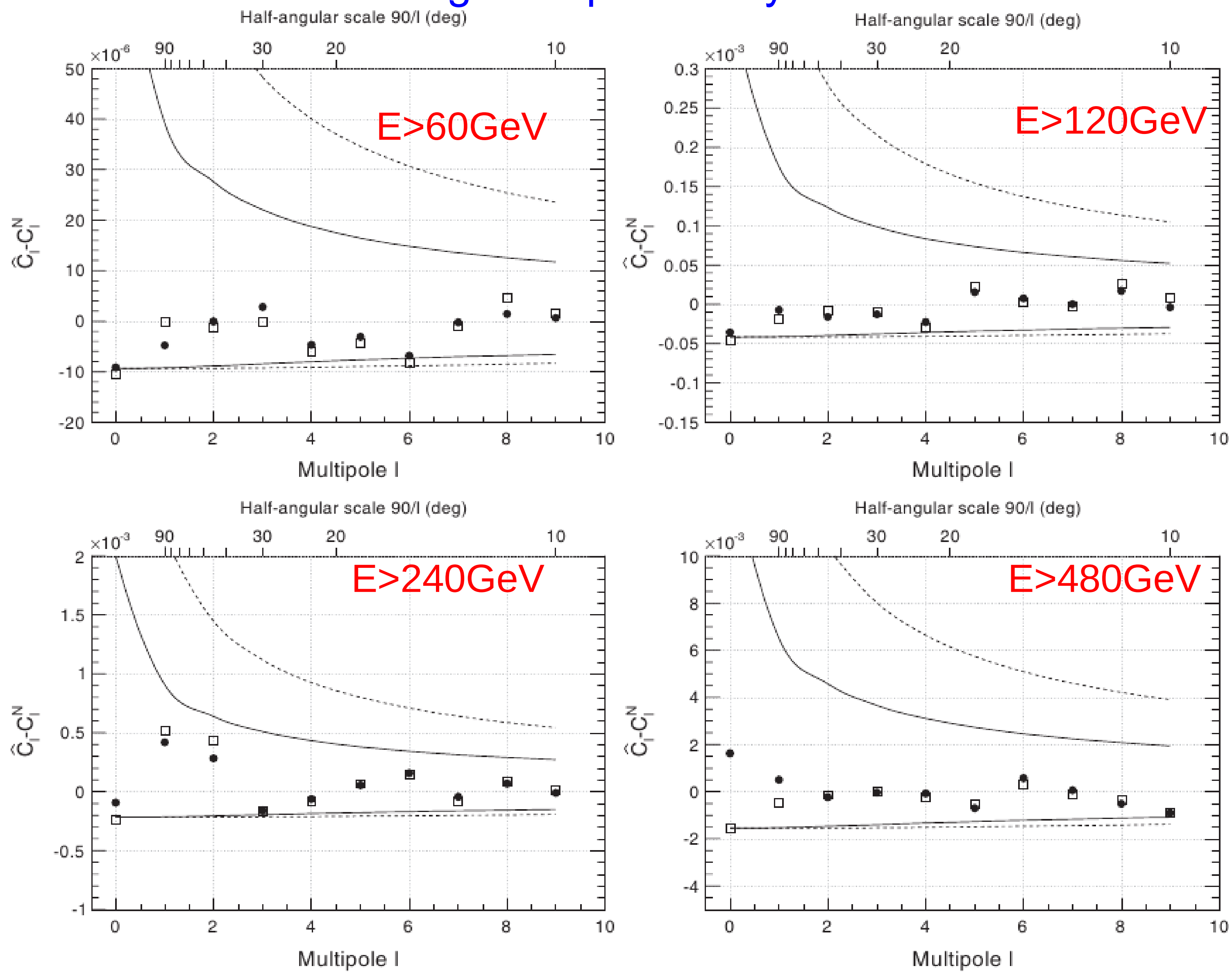

- The presence of any anisotropies would make the markers rise over these curves.
- **The spectra are consistent with being mere statistical fluctuations of an isotropic signal.**

Upper Limits from the Harmonic Analysis

- **Markers**: 90% and 95% C.L. upper limits on the dipole anisotropy as produced by the spherical harmonic analysis.
- In general: $\delta=(I_{max}-I_{min})/(I_{max}+I_{min})$. For a dipole $I(\theta)=I_0+I_1{}^*\cos(\theta) \rightarrow \delta=I_1/I_0$

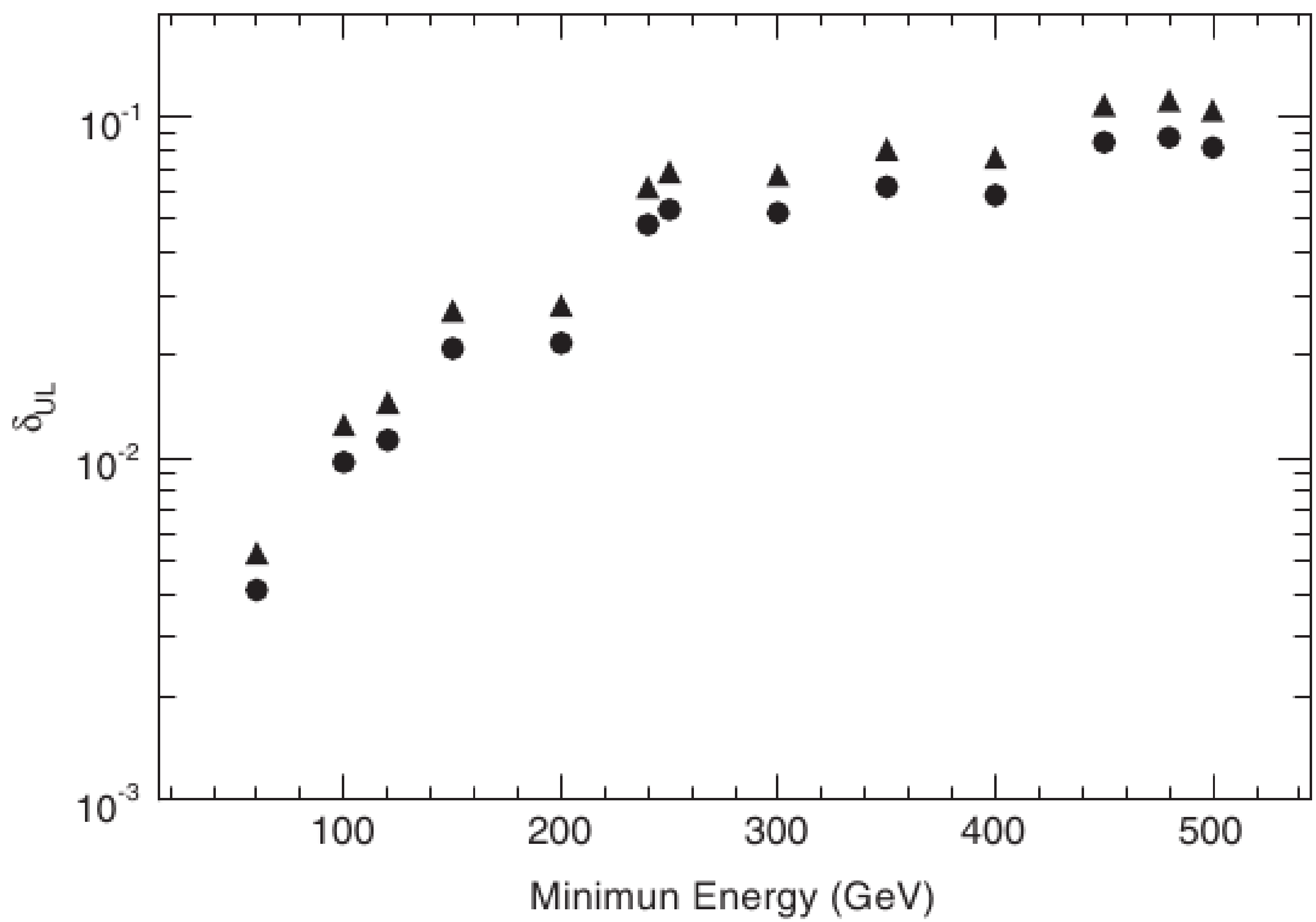

Anisotropy from individual sources

- CRE spectrum hard to fit with a single-component diffusive model. With the addition of a nearby e^-e^+ source (e.g. a pulsar) we can fit both the CRE spectrum and the Pamela positron-fraction results.

➢ We used a GALPROP simulation to evaluate the spectrum at the earth caused by a single (assumed as) dominant nearby source: Vela or Monogem.

  - The source luminosity was set up such as the resulting spectrum does not exceed the flux measured by *Fermi*-LAT and H.E.S.S.
  - For each source, the anisotropy has been evaluated assuming that the contributions to the anisotropy from all remaining sources were negligible.

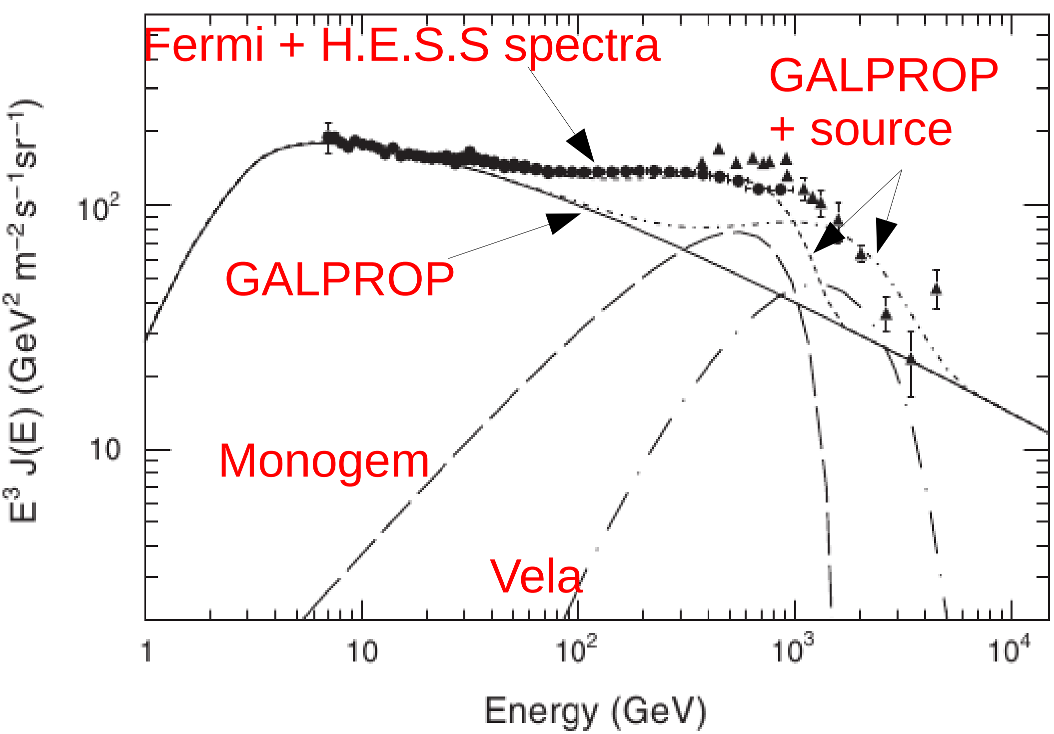

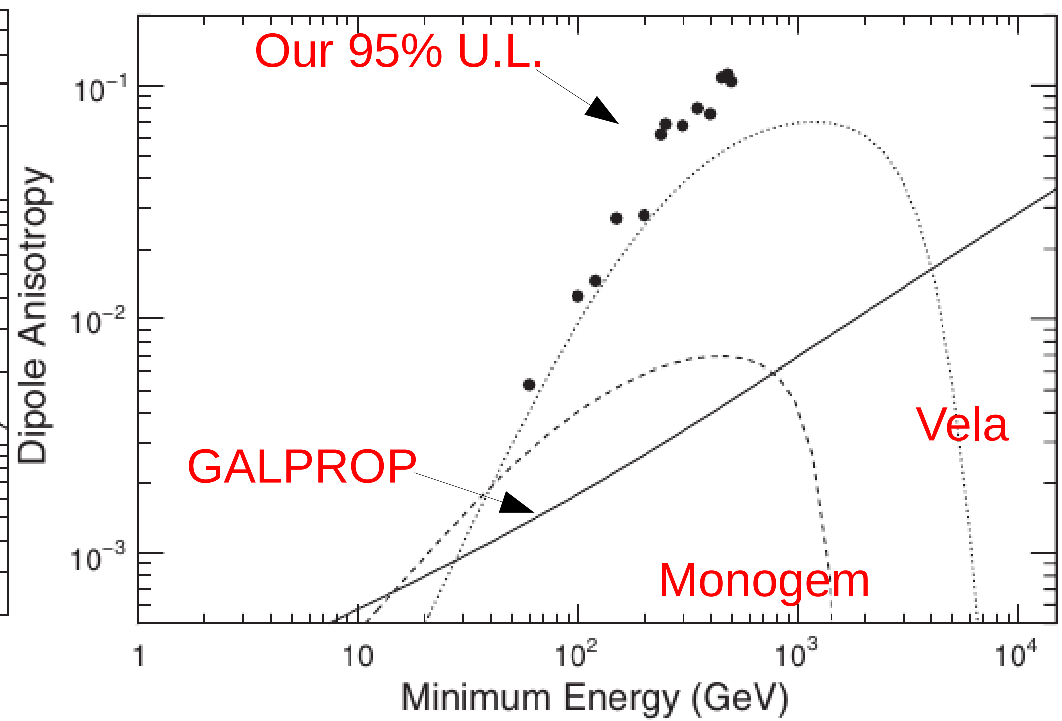

Interpretation #2 – Dark Matter

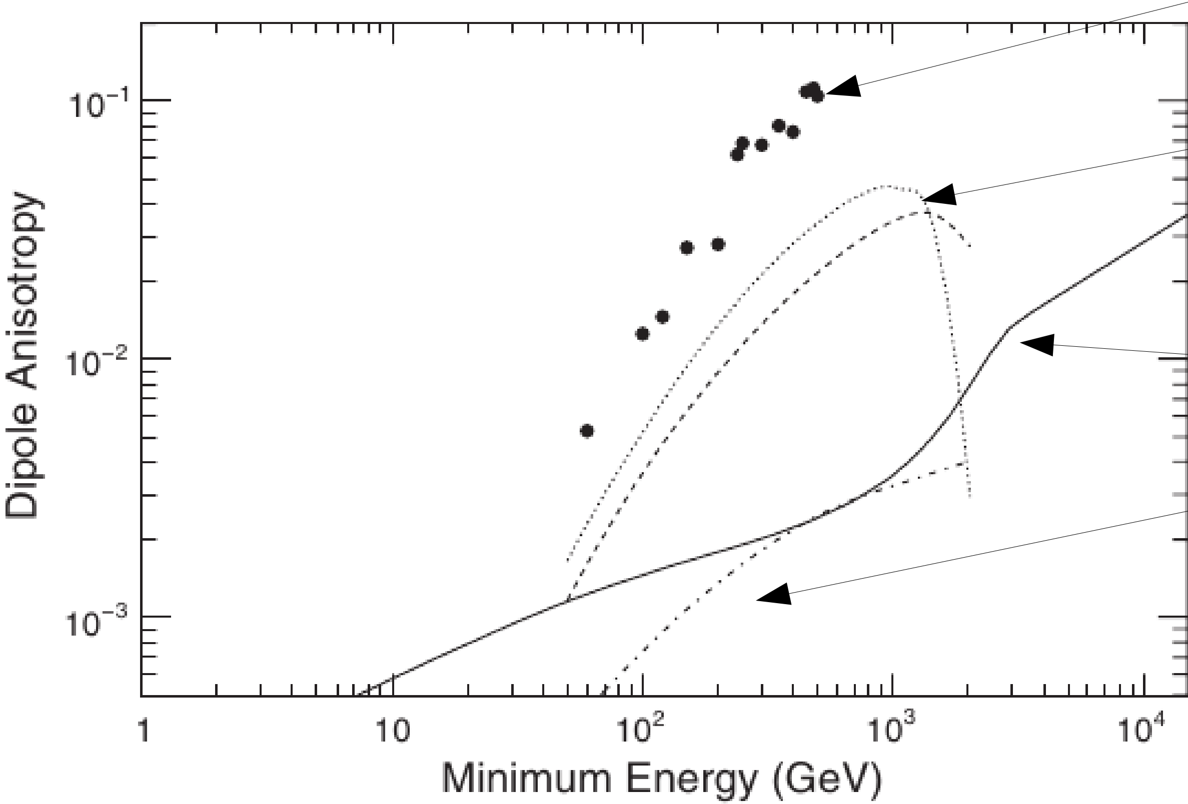

- **Dots:** Our 95% upper limits on the dipole anisotropy.
- **Dashed (dotted) line** (1): Single DM clump moving away (towards) us.
- **Solid line** (2): DM distributed in the Milky Way halo.
- **Dot-dashed line** (3): DM from a population of galactic substructures.
- ***These DM models were tuned to match Fermi & Pamela results.***

- **(1)**: 300 km/s speed perpendicular to the galactic plane, 5 (3) TeV mass, departing at 1.54 kpc (approaching at 1.43 kpc). From Regis & Ullio 2009.
- **(2)**: NFW profile, 3 TeV mass DM → $\tau^+\tau^-$, DM density 0.43 GeV/cm^3, 20kpc core radius
- **(3)**: NFW profile, 3.6 TeV mass DM → $\tau^+\tau^-$. From Cernuda 2010.
- *NFW: Navarro, Frenk, White*

Conclusion

- A search for anisotropies in the incoming directions of 1-year worth of CRE data detected by the *Fermi*-LAT resulted to no detections.
- We placed upper limits on the degree of anisotropy and provided some interpretation of our results in the contexts of a nearby e^-e^+ source (pulsar) and DM.
- See our paper at Ackermann et al. Phys.Rev.D82:092003,2010
- http://arxiv.org/abs/1008.5119

THANK YOU!

- Using the diffusion approximation in Ginzburg & Ptuskin 1976 with N the density of particles and D the diffusion coefficient:

$$\delta = \frac{3D}{c}\frac{|\vec{\nabla} N|}{N}$$

- For a pure diffusive model and by solving the transport equation: (r_{diff} is the diffusion distance)

$$\delta_i = \frac{3D}{c}\frac{2|\vec{r}_i|}{r_{\rm diff}^2}$$

- For E<<E_{max} $r_{\rm diff} \simeq 2\sqrt{Dt_i}$, where t_i is the age of the source and:

$$\delta_i = \frac{3|\vec{r}_i|}{2ct_i}.$$

- For a distribution of sources:

$$\delta = \frac{\sum_i N_i \delta_i \hat{r}_i \cdot \hat{n}_{\rm max}}{\sum_i N_i},$$

Calculation

- Electron injection spectrum for summed sources: broken power-law γ=1.6 (2.7) below)(above) 4GeV.
- $D(E) = D_0(\frac{E}{E_0})^{0.33}$, where $D_0 = 5.8 \times 10^{28}$ cm^2 s^{-1} 30k $E_0 = 4$ GeV
- Halo height 4kpc
- Vela 290pc distance and 1.1x10^4 yr age, Monogem 290pc distance and 1.1x10^5 age
- For the single sources we adopted a burst-like spectrum in which duration of emission << travel time to the source.
  - Power law with exponential cutoff: Γ=1.7, E_{cut}=1.1TeV
- Spectrum of CREs at solar system:

$$N(E, t_i, \vec{r}_i) = \frac{Q_0}{\pi^{3/2} r_{\rm diff}^3}\left(1 - \frac{E}{E_{\rm max}}\right)^{\Gamma-2}\left(\frac{E}{1\ {\rm GeV}}\right)^{-\Gamma} \times \exp\left(-\frac{E}{(1-\frac{E}{E_{\rm max}})E_{\rm cut}}\right)\exp\left(-\frac{r_i^2}{r_{\rm diff}^2}\right).$$

- The normalization constant Q_o was tuned so that the individual-source spectra no exceed our measurements.

TABLE I. Geometry factor, residual contamination, number of counts before background subtraction, and the flux J_E multiplied by E^3. The statistical error is followed by the systematic error. The latter does not include the effect due to the uncertainty in the absolute energy scale (see text).

Energy (GeV)	GF (m^2 sr)	Residual contamination	Counts	$E^3 J_E$ ($GeV^2\ s^{-1}\ m^{-2}\ sr^{-1}$)
23.6–26.0	1.65	0.04	478 929	$151.6 \pm 1.2^{+7.3}_{-8.3}$
26.0–28.7	2.03	0.05	502 083	$152.6 \pm 0.9^{+6.2}_{-7.3}$
28.7–31.7	2.35	0.05	487 890	$151.4 \pm 0.8^{+5.1}_{-6.5}$
31.7–35.0	2.59	0.09	459 954	$151.3 \pm 1.8^{+5.2}_{-6.5}$
35.0–38.8	2.67	0.07	385 480	$149.6 \pm 0.7^{+4.4}_{-5.8}$
38.8–43.1	2.72	0.08	330 061	$150.2 \pm 0.7^{+4.5}_{-6.0}$
43.1–48.0	2.76	0.10	276 105	$148.6 \pm 0.7^{+4.9}_{-6.2}$
48.0–53.7	2.79	0.11	233 877	$146.5 \pm 0.7^{+4.9}_{-6.1}$
53.7–60.4	2.77	0.12	194 062	$145.5 \pm 0.7^{+5.0}_{-7.1}$
60.4–68.2	2.76	0.13	155 585	$143.2 \pm 0.7^{+5.6}_{-6.8}$
68.2–77.4	2.73	0.14	126 485	$141.9 \pm 0.8^{+5.6}_{-7.0}$
77.4–88.1	2.71	0.14	100 663	$140.8 \pm 0.8^{+6.2}_{-7.0}$
88.1–101	2.68	0.15	77 713	$139.0 \pm 0.9^{+6.4}_{-6.8}$
101–116	2.64	0.16	61 976	$139.0 \pm 0.9^{+6.4}_{-7.2}$
116–133	2.58	0.17	46 865	$139.4 \pm 1.0^{+6.9}_{-7.2}$
133–154	2.52	0.17	35 105	$139.5 \pm 1.2^{+7.2}_{-7.4}$
154–180	2.44	0.17	27 293	$140.8 \pm 1.3^{+6.9}_{-7.4}$
180–210	2.36	0.18	19 722	$142.3 \pm 1.5^{+7.1}_{-7.4}$
210–246	2.27	0.18	13 919	$140.9 \pm 1.7^{+7.4}_{-6.8}$
246–291	2.14	0.18	10 019	$140.9 \pm 1.9^{+7.5}_{-6.7}$
291–346	2.04	0.18	7207	$140.4 \pm 2.2^{+6.7}_{-7.0}$
346–415	1.88	0.18	4843	$139.4 \pm 2.6^{+7.0}_{-7.2}$
415–503	1.73	0.19	3036	$134.0 \pm 3.1^{+9.3}_{-7.5}$
503–615	1.54	0.20	1839	$127.4 \pm 4.1^{+8.7}_{-8.6}$
615–772	1.26	0.21	1039	$115.8 \pm 4.8^{+15.2}_{-10.9}$
772–1000	0.88	0.21	544	$114.4 \pm 6.5^{+19.1}_{-17.8}$

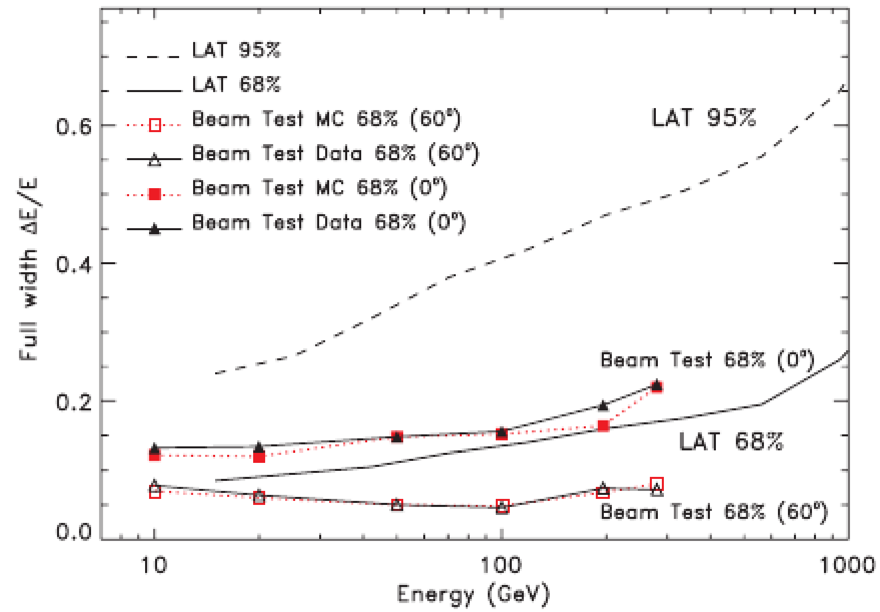

FIG. 1 (color online). Energy resolution for the LAT after electron selection; the full widths of the smallest energy window containing the 68% and the 95% of the energy dispersion distribution are shown. The comparison with beam test data up to 282 GeV and for on-axis and at 60° incidence shown in the figure indicates good agreement with the resolution estimated from the simulation.

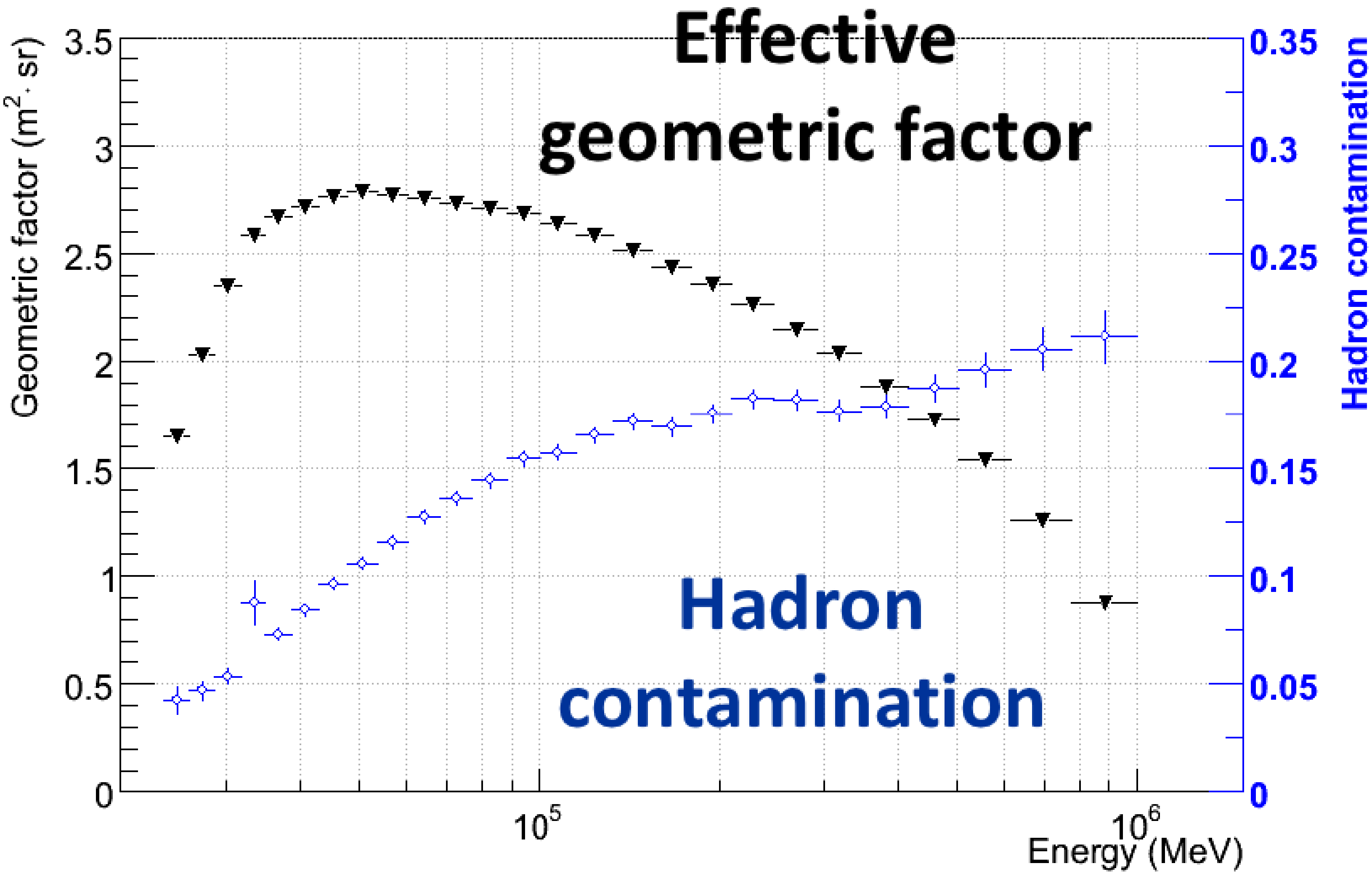

Effective
geometric factor
Hadron
contamination
Geometric factor (m$^2 \cdot$ sr)
3.5
3
2.5
2
1.5
1
0.5
0
Hadron contamination
0.35
0.3
0.25
0.2
0.15
0.1
0.05
0
10^5
10^6
Energy (MeV)